

**HWR No. 04-01**

**Characterization of Aquifer  
Heterogeneity Using Transient  
Hydraulic Tomography**

by

Junfeng Zhu  
and  
Tian-Chyi J. Yeh

Department of Hydrology and Water Resources  
University of Arizona  
Tucson Arizona 85721

November 2004

1

2

3

4

5

Characterization of Aquifer Heterogeneity Using Transient

6

Hydraulic Tomography

7

8

By

9

10

Junfeng Zhu and Tian-Chyi J. Yeh

11

12

13

Department of Hydrology and Water Resources

14

The University of Arizona

15

Tucson, Arizona 85721

16

November 2004

1

**2 Abstract**

3       Hydraulic tomography is a cost-effective technique for characterizing the  
4 heterogeneity of hydraulic parameters in the subsurface. During hydraulic tomography  
5 surveys, a large number of hydraulic heads (i.e., aquifer responses) are collected from a  
6 series of pumping or injection tests in an aquifer. These responses are then used to  
7 interpret the spatial distribution of hydraulic parameters of the aquifer using inverse  
8 modeling. In this study, we developed an efficient sequential successive linear estimator  
9 (SSLE) for interpreting data from transient hydraulic tomography to estimate three-  
10 dimensional hydraulic conductivity and specific storage fields of aquifers. We first  
11 explored this estimator for transient hydraulic tomography in a hypothetical one-  
12 dimensional aquifer. Results show that during a pumping test, transient heads are highly  
13 correlated with specific storage at early time but with hydraulic conductivity at late time.  
14 Therefore, reliable estimates of both hydraulic conductivity and specific storage must  
15 exploit the head data at both early and late times. Our study also shows that the transient  
16 heads are highly correlated over time, implying only infrequent head measurements are  
17 needed during the estimation. Applying this sampling strategy to a well-posed problem,  
18 we show that our SSLE can produce accurate estimates of both hydraulic conductivity  
19 and specific storage fields. The benefit of hydraulic tomography for ill-posed problems  
20 is then demonstrated. Finally, to affirm the robustness of our SSLE approach, we apply  
21 the SSLE approach to transient hydraulic tomography in a hypothetical two-dimensional  
22 aquifer with nonstationary hydraulic properties, as well as a hypothetical three-  
23 dimensional heterogeneous aquifer.

- 1 Key words: *transient hydraulic tomography, SSLE, cokriging, temporal correlation,*
- 2 *hydraulic conductivity, specific storage.*
- 3

## 1 **1. Introduction**

2 Detailed spatial distributions of hydraulic parameters are imperative to improve  
3 our ability to predict water and solute movement in the subsurface (e.g., Yeh, 1992, 1998).  
4 Traditional aquifer tests like pumping tests and slug tests only yield hydraulic parameters  
5 integrated over a large volume (e.g., Butler and Liu, 1993). Furthermore, the study by  
6 Wu et al. (2004) reports that the classical analysis for aquifer tests yields unrepresentative  
7 estimates of transmissivity and storage coefficient. For characterizing detailed spatial  
8 distributions of hydraulic parameters, a new method, hydraulic tomography (Gottlieb and  
9 Dietrich, 1995; Renshaw, 1996; Yeh and Liu, 2000; Liu et al., 2002; McDermott et al.,  
10 2003), which evolved from the CAT scan concept of medical sciences and geophysics,  
11 appears to be a viable technology.

12 Hydraulic tomography is, in the most simplified terms, a series of cross-well  
13 influence tests. In other words, an aquifer is stressed by pumping water from or injecting  
14 water into a well, and monitoring the aquifer's response at other wells. A set of  
15 stress/response yields an independent set of equations. Sequentially switching the  
16 pumping or injection location, without installing additional wells, results in a large  
17 number of aquifer responses caused by stresses at different locations and, in turn, a large  
18 number of independent sets of equations. This large number of sets of equations makes  
19 the inverse problem (i.e., using aquifer stress and response relation to estimate the spatial  
20 distribution of hydraulic parameters) better posed, and the subsequent estimate  
21 approaches reality.

22 Interpreting data from hydraulic tomography presents a challenge, however. The  
23 abundance of data generated during tomography can lead to information overload, and

1 cause substantial computational burdens and numerical instabilities (Yeh, 1986, Hughson  
2 and Yeh, 2000). Moreover, the interpretation can be non-unique. Yeh and Liu (2000)  
3 developed a sequential successive linear estimator (SSLE) to overcome these difficulties.  
4 The SSLE approach eases the computational burdens by sequentially including  
5 information obtained from different pumping tests; it resolves the non-uniqueness issue  
6 by providing the best unbiased conditional mean estimate. That is, it conceptualizes  
7 hydraulic parameter fields as spatial stochastic processes and seeks their mean  
8 distributions conditioned on the information obtained from hydraulic tomography, as well  
9 as directly measured parameter values (such as from slug tests, or core samples). Using  
10 sand box experiments, Liu et al. (2002) demonstrated that the combination of hydraulic  
11 tomography and SSLE is a propitious, cost-effective technique for delineating  
12 heterogeneity using a limited number of invasive observations. The work by Yeh and Liu  
13 (2000), nonetheless, is limited to steady state flow conditions, which may occur only  
14 under special field conditions. Because of this restriction, their method ignores transient  
15 head data before flow reaches steady state conditions. Transient head data, although  
16 influenced by both hydraulic conductivity and specific storage, are less likely to be  
17 affected by uncertainty in boundary conditions. The development of a new estimation  
18 procedure thus becomes essential such that all datasets collected during hydraulic  
19 tomography surveys can be fully exploited.

20 Few researchers have investigated transient hydraulic tomography. For example,  
21 Bohling et al. (2002) exploited the steady-shape flow regime of transient flow data to  
22 interpret tomographic surveys. Under steady-shape conditions at late time of a pumping  
23 test before boundary effects take place, the hydraulic gradient changes little with time--a

1 situation where sensitivity of head to the specific storage is small. As a consequence, the  
2 steady-shape method is useful for estimating hydraulic conductivity but not specific  
3 storage.

4 Their steady-shape method relies on the classical least-squares optimization  
5 method and the Levenberg-Marquardt algorithm (Marquardt, 1963) for controlling  
6 convergence issues (see Nowak and Cirpka, 2004). This optimization method is known  
7 to suffer from non-uniqueness of the solutions if the inverse problem is ill posed and  
8 regularization (Tikhonov and Arsenin, 1977) or prior covariance of parameters (Nowak  
9 and Cirpka, 2004) is not used. The least-squares approach is also computationally  
10 inefficient if every element in the solution domain (in particular, three-dimensional  
11 aquifers with multiple, randomly distributed parameters) is to be estimated. This  
12 inefficiency augments if the sensitivity matrices required by the optimization are not  
13 evaluated using an efficient algorithm, such as the adjoint state approach.

14 These shortcomings may be the reasons that test cases in Bohling et al. (2002)  
15 were restricted to unrealistic, perfectly stratified aquifers, where the heterogeneity has no  
16 angular variations, and specific storage is constant and known a priori. The assumption  
17 of a spatially constant and known specific storage value for the entire aquifer makes the  
18 inverse problem almost the same as the steady hydraulic tomography as explored by Yeh  
19 and Liu (2000). Perhaps the inverse problem of the transient tomography is less affected  
20 by unknown in boundary conditions. Lastly, for perfectly horizontal layered aquifers,  
21 many traditional hydraulic test methods, without resorting to hydraulic tomography, can  
22 easily estimate hydraulic properties of each layer using just one borehole.

1            Similar to Vasco et al. (2000), Brauchler et al. (2003) developed a method that  
2 uses the travel time of a pneumatic pressure pulse to estimate air diffusivity of fractured  
3 rock. Similar to X-ray tomography, their approach relies on the assumption that the  
4 pressure pulse travels along a straight line. Thus, an analytical solution can be derived for  
5 the propagation of the pressure pulse between a source and a pressure sensor. Many pairs  
6 of sources and sensors yield a system of one-dimensional analytical equations. A least-  
7 squares based inverse procedure developed for seismic tomography can then be applied  
8 to the system of equations to estimate the diffusivity distribution. The ray approach  
9 avoids complications involved in numerical formulation of the three-dimensional forward  
10 and inverse problems, but it ignores interaction between adjacent ray paths and possible  
11 boundary effects. Consequently, their method requires an extensive number of iterations  
12 and pairs of source/sensor data to achieve a comparable resolution to that achieved from  
13 inverting a three-dimensional model.

14            To our knowledge, no researchers have developed an inverse method for transient  
15 hydraulic tomography to estimate both hydraulic conductivity and specific storage of  
16 aquifers. For general groundwater inverse problems other than hydraulic tomography,  
17 Sun and Yeh (1992) assumed a specific storage field that was homogeneous and known a  
18 priori. They then developed a stochastic inverse method to estimate the spatial  
19 distribution of transmissivity using only transient head information. For transient  
20 hydraulic tomography, Vasco et al. (2000) and Brauchler et al. (2003) estimated  
21 diffusivity, the ratio of hydraulic conductivity to specific storage, without any attempt to  
22 separate the two parameters.



1           In this paper, we extended the SSLE developed by Yeh and Liu (2000) to  
 2 transient hydraulic tomography for estimating randomly distributed hydraulic  
 3 conductivity and specific storage in 3-D aquifers. This paper begins with the derivation  
 4 of the SSLE for use with transient hydraulic heads. We introduce a loop iteration scheme  
 5 to improve the accuracy of sequential usage of head data. We then verify our new  
 6 approach by applying it to a synthetic one-dimensional heterogeneous aquifer. During  
 7 this one-dimensional test, temporal variation of cross-correlation between transient heads  
 8 and parameters, as well as temporal correlation of transient heads, is investigated. Results  
 9 of this investigation lead to an effective sampling strategy, as opposed to developing an  
 10 entire well hydraulic graph as used by Bohling et al. (2002), for efficient inversion of the  
 11 transient hydraulic tomography data. To clarify the common myth about the stationary  
 12 stochastic process assumption behind the SSLE approach (e.g., Kosugi and Inoue, 2002),  
 13 we subsequently apply our new approach to a transient hydraulic tomographic survey in a  
 14 hypothetical, two-dimensional nonstationary aquifer. Finally, the new SSLE is applied  
 15 to a hypothetical three-dimensional, heterogeneous aquifer to demonstrate the robustness  
 16 of our new approach.

17

## 18 **2. Method**

### 19 2.1 Groundwater Flow in Three-dimensional Saturated Media

20           In the following analysis, we assume that groundwater flow in three-dimensional,  
 21 saturated, heterogeneous, porous media can be described by the following equation:

$$22 \quad \nabla \cdot [K(x)\nabla H] + Q(x) = S_s(x) \frac{\partial H}{\partial t} \quad (1)$$

23 subject to boundary and initial conditions:

$$1 \quad H|_{\Gamma_1} = H_1, \quad [K(\mathbf{x})\nabla H] \cdot \mathbf{n}|_{\Gamma_2} = q, \quad \text{and} \quad H|_{t=0} = H_0 \quad (2)$$

2 where in (1),  $H$  is total head (L),  $\mathbf{x}$  is the spatial coordinate ( $\mathbf{x} = \{x_1, x_2, x_3\}$ , (L), and  $x_3$   
 3 represents the vertical coordinate and is positive upward),  $Q(\mathbf{x})$  is the pumping rate (1/T)  
 4 at the location  $\mathbf{x}$ ,  $K(\mathbf{x})$  is the saturated hydraulic conductivity (L/T), and  $S_s(\mathbf{x})$  is the  
 5 specific storage ( $L^{-1}$ ). In equation (2),  $H_1$  is the prescribed total head at Dirichlet  
 6 boundary  $\Gamma_1$ ,  $q$  is the specific flux (L/T) at Neumann boundary  $\Gamma_2$ ,  $\mathbf{n}$  is a unit vector  
 7 normal to the union of  $\Gamma_1$  and  $\Gamma_2$ , and  $H_0$  represents the initial total head. The equation is  
 8 solved by a 3-D finite element approach developed by Srivastava and Yeh (1992) in the  
 9 following analysis.

10

## 11 2.2 Sequential Successive Linear Estimator (SSLE)

12 The SSLE approach is an extension of the SLE (Successive Linear Estimator)  
 13 approach (Yeh et al., 1996; Zhang and Yeh, 1997; Hanna and Yeh, 1998; Vargas-  
 14 Guzman and Yeh, 1999, 2002; Hughson and Yeh, 2000). The SLE approach is  
 15 essentially cokriging (Yeh et al., 1995)--Bayesian formalism (Kitanidis, 1986)--that seeks  
 16 mean parameter fields conditioned on available point data as well as geological and  
 17 hydrologic structures (i.e., spatial covariance functions of parameters and hydraulic heads,  
 18 and their cross-covariance functions). Different from cokriging, SLE uses a linear  
 19 estimator successively to update both conditional means and covariances such that the  
 20 nonlinear relation between information and parameters is considered. As a stochastic  
 21 estimator analogous to the direct method of the deterministic approach (see Yeh, 1986),  
 22 SLE is different from the maximum a posterior (McLaughlin and Townley, 1996) and the  
 23 quasi-linear geostatistical inverse approach (Kitanidis, 1995). The latter are merely least-

1 squares optimization algorithms using the kriging or cokriging estimate as an initial guess  
 2 and parameter covariances for regularization.

3 The SSLE approach relies on the SLE concept to sequentially include data sets  
 4 and update covariances and cross-covariances in the estimation process. The sequential  
 5 method avoids solving huge systems of equations and therefore reduces numerical  
 6 difficulties. The approach has been successfully applied to parameter estimations in  
 7 variably saturated media (e.g., Zhang and Yeh, 1997; Hanna and Yeh, 1998; Hughson  
 8 and Yeh, 2000), steady hydraulic tomography (Yeh and Liu, 2000; Liu et al., 2002),  
 9 electrical resistivity tomography (Yeh et al., 2002); and stochastic information fusion  
 10 (Yeh and Šimůnek, 2002; Liu and Yeh, 2004). In this study, we extend this inverse  
 11 approach to incorporate transient hydraulic head data to estimate both hydraulic  
 12 conductivity and specific storage fields. As the majority of the SSLE method used in this  
 13 study remains similar to that in previous works by Yeh and his colleagues, we present  
 14 only a brief summary, but a sensitivity analysis for transient flow, and a new loop  
 15 iteration scheme are given in detail below.

16 To characterize the heterogeneity of geological formations, the SSLE algorithm  
 17 treats the natural logs of saturated hydraulic conductivity and specific storage as  
 18 stochastic processes. We therefore assume  $\ln K = \bar{K} + f$  and  $\ln S_s = \bar{S} + s$ , where  $\bar{K}$  and  $\bar{S}$   
 19 are mean values, and  $f$  and  $s$  denote the perturbations. The transient hydraulic head  
 20 response to a pumping test in transient hydraulic tomography is represented by  $H = \bar{H} + h$ ,  
 21 where  $\bar{H}$  is the mean and  $h$  is the perturbation. Substituting these stochastic variables  
 22 into (1), taking the conditional expectation, and conditioning with some observations of  
 23 head and parameters generates the mean flow equation as

$$1 \quad \nabla \cdot [\bar{K}_{con}(\mathbf{x}) \nabla \bar{H}_{con}] + Q = \bar{S}_{con}(\mathbf{x}) \frac{\partial \bar{H}_{con}}{\partial t} \quad (3)$$

2 where  $\bar{K}_{con}$ ,  $\bar{H}_{con}$ , and  $\bar{S}_{con}$  are conditional effective hydraulic conductivity, hydraulic  
 3 head and specific storage, respectively, and  $Q$  is the pumping rate at a given location,  
 4 which is known a priori. Similar to the work by Yeh and his colleagues, we seek the  
 5 conditional effect fields of hydraulic conductivity and specific storage, conditioned on the  
 6 information from transient hydraulic tomography and some direct measurements of  $K$  and  
 7  $S_s$ .

8 The estimation procedure starts with a weighted linear combination of direct  
 9 measurements of the parameters and transient head data at different locations to obtain  
 10 the first estimate of the parameters. The weights are calculated based on statistical  
 11 moments (namely, means, and covariances) of parameters, the covariances of heads,  
 12 cross-covariances between heads and parameters, and cross-covariance of heads at  
 13 different times. The first estimate is then used in the mean flow equation to calculate  
 14 the head at observation locations and sampling times (i.e., forward simulation).  
 15 Differences between the observed and simulated heads are determined subsequently. A  
 16 weighted linear combination of these differences is then used to improve the previous  
 17 estimates. Iterations between the forward simulation and estimation continue until the  
 18 improvement in the estimates diminishes to a prescribed value.

19

#### 20 a) Sensitivity analysis of transient flow

21 In the above estimation procedure, the head covariance in space and time and its  
 22 cross-covariances with parameters are evaluated using a first-order approximation, which  
 23 involves evaluation of sensitivity matrices of the governing flow equation. The

1 sensitivity matrices are evaluated as follows. Transient hydraulic heads are expanded in  
 2 a Taylor series around the mean values of parameters. After neglecting second and higher  
 3 order terms, the transient hydraulic head is:

$$4 \quad H = \bar{H} + f \left. \frac{\partial H}{\partial f} \right|_{\bar{k}, \bar{H}} + s \left. \frac{\partial H}{\partial s} \right|_{\bar{s}, \bar{H}} \quad (4)$$

5 The sensitivity terms  $\left. \frac{\partial H}{\partial f} \right|_{\bar{k}, \bar{H}}$  and  $\left. \frac{\partial H}{\partial s} \right|_{\bar{s}, \bar{H}}$  in (4) are calculated by the adjoint state  
 6 method (Sykes, et al. 1985; Li and Yeh, 1998). We briefly describe the method here  
 7 (refer to Li and Yeh (1998, 1999), Sun and Yeh (1992) for a detailed derivation). The  
 8 marginal sensitivity of a performance measure  $P$  to a parameter  $\chi$  is defined as

$$9 \quad \frac{dP}{d\chi} = \int_T \int_{\Omega} \left( \frac{\partial G}{\partial \chi} + \frac{\partial G}{\partial H} \frac{\partial H}{\partial \chi} \right) d\Omega dt \quad (5)$$

10 where  $T$  and  $\Omega$  represent time and spatial domain, respectively. The first term of the  
 11 integral in (5) indicates the direct dependence of  $P$  on  $\chi$ , while the second term indicates  
 12 the implicit dependence of  $P$  on  $\chi$  through the heads (Sykes et al., 1985). In this case,

$$13 \quad G = H \delta(x - x_k)(t - t_l) \quad (6)$$

14 representing the hydraulic head at location  $x_k$  and time  $t_l$ , where  $\delta$  is Kronecker delta-  
 15 function which equals unity if  $x$  equals  $x_k$  and  $t$  equals  $t_l$ , and equals zero otherwise.

16 Differentiating (1) with respect to a parameter  $\chi$ , multiplying by a arbitrary  
 17 function  $\phi^*$ , integrating over  $T$  and  $\Omega$ , applying Green's Identities, and dropping  
 18 boundary terms gives

$$19 \quad \int_T \int_{\Omega} \left[ \frac{\partial S}{\partial \chi} \frac{\partial H}{\partial t} \phi^* + \frac{\partial K}{\partial \chi} \nabla H \nabla \phi^* - \phi S \frac{\partial \phi^*}{\partial t} - \phi \nabla \cdot (K \nabla \phi^*) \right] d\Omega dt + \int_{\Omega} S \phi^* \phi d\Omega \Big|_{t=0}^{t=T} = 0 \quad (7)$$

1 where  $\phi = \partial H / \partial \chi$  is the sensitivity of  $H$  to  $\chi$  and is called state sensitivity, and  $T_e$  is the  
 2 final simulation time. Adding (7) to the right hand side of (5), and substituting (6) for  $G$ ,  
 3 we have

$$\begin{aligned}
 \frac{dP}{d\chi} = & \int_T \int_{\Omega} [\phi \delta(x - x_k)(t - t_l) + \frac{\partial S}{\partial \chi} \frac{\partial H}{\partial t} \phi^* + \frac{\partial K}{\partial \chi} \nabla H \nabla \phi^* - \phi S \frac{\partial \phi^*}{\partial t} - \phi \nabla \cdot (K \nabla \phi^*)] d\Omega dt \\
 & + \int_{\Omega} S \phi^* \phi d\Omega \Big|_{t=0}^{t=T_e}
 \end{aligned} \tag{8}$$

5 We then choose the arbitrary function  $\phi^*$  that satisfies

$$S \frac{\partial \phi^*}{\partial t} + \nabla \cdot (K \nabla \phi^*) - \delta(x - x_k)(t - t_l) = 0 \tag{9}$$

7 with boundary and final conditions:

$$\phi^* \Big|_{\Gamma_1} = 0, \quad [K(\mathbf{x}) \nabla \phi^*] \cdot \mathbf{n} \Big|_{\Gamma_2} = 0, \quad \phi^* \Big|_{t=T_e} = 0 \tag{10}$$

9 (note that (9) and (10) are called adjoint state equations); we further assume that the  
 10 initial condition is known a priori, such that  $\phi \Big|_{t=0} = 0$ , and hydraulic conductivity and  
 11 specific storage are not correlated to each other. Thus, the sensitivities of the hydraulic  
 12 head at location  $x_k$  and time  $t_l$  to  $f$  and  $s$  are given by

$$\frac{dH}{df_k} = \int_T \int_{\Omega_k} \left\{ \frac{\partial K}{\partial f_k} \frac{\partial \phi^*}{\partial x_i} \frac{\partial H}{\partial x_i} \right\} dt d\Omega_k \tag{11}$$

$$\frac{dH}{ds_k} = \int_T \int_{\Omega_k} \left\{ \frac{\partial S}{\partial s_k} \phi^* \frac{\partial H}{\partial t} \right\} dt d\Omega_k \tag{12}$$

15 where  $f_k$  and  $s_k$  are the perturbations of  $K$  and  $S$  at element  $k$  when the study domain is  
 16 discretized. Note that the adjoint state equations are also transient problems and need to  
 17 be solved backwardly in time. Also, the mean transient hydraulic heads must be derived  
 18 beforehand in order to evaluate the sensitivities. The mean flow equation is given by

1 equation (3). After  $\phi^*$  and the mean head are calculated, the sensitivities obtained from  
2 equations (11) and (12) can be used to calculate covariances and cross-covariances.

3

#### 4 b) Loop iteration scheme

5           As indicated by Vargas-Guzman and Yeh (2002) and Yeh and Šimůnek (2002)  
6 in previous SSLE approaches, the method of adding different data sets sequentially works  
7 best for linear systems. The relations between transient head and hydraulic parameters,  
8 however, are nonlinear; the sequential approach cannot fully exploit the head information.  
9 For instance, assume two datasets, A and B, are used in an inversion problem. The B  
10 dataset is added after the A dataset reaches convergence. The SSLE then stops after the B  
11 dataset converges. While the final estimates meet the convergence criteria for the B  
12 dataset, they may not now meet the convergence criteria for the A dataset. In addition,  
13 adding datasets in different sequences may lead to different results. Therefore, we  
14 introduced a new loop iteration scheme.

15           In this loop iteration scheme, the next dataset is added after all the datasets  
16 already incorporated meet the converge criteria within one loop. Specifically, a dataset is  
17 fed into SSLE first, and SSLE then iterates until this dataset meets a converge criterion. A  
18 new dataset is added afterwards, and SSLE again iterates until the new estimate  
19 convergences. Instead of adding the next new dataset, the scheme goes back to check the  
20 convergence for the first dataset. If the converge criterion is not met. The program starts a  
21 loop iteration in which the iteration involves both the first and second datasets. That is,  
22 the first dataset is iterated once, and then the second dataset is incorporated and iterated  
23 once also; we call this process a loop. The loop iteration continues until both datasets

1 meet the converge criterion within one loop. Then, the next new dataset is added. The  
2 algorithm treats this new dataset similarly to the second dataset, except the loop iteration  
3 now involves three datasets. Additional datasets are added in a similar way. As a  
4 consequence, our inverse approach improves estimates throughout the loops, maximizes  
5 the usefulness of datasets, and alleviates the problems associated with the previous SSLE  
6 approach used by Yeh and his colleagues.

7       During a transient pumping test, one can record a large number of head observations  
8 at different times. As stated by Sun and Yeh (1992), simultaneous inclusion of transient  
9 head data at different times improves the estimates and decreases the head misfit because  
10 simultaneous inclusion considers the temporal correlation of transient heads. In our  
11 approach, we included in the estimation all observed heads at different times during a  
12 pumping activity. The head responses from different pumping tests are included  
13 sequentially.

14

### 15 **3. Numerical Examples**

#### 16 **3.1 One-Dimensional Flow**

17       To test our inverse approach, a hypothetical, one-dimensional, horizontal,  
18 heterogeneous, confined aquifer was used. The aquifer was 20 meters long and was  
19 discretized into twenty elements. Each element was one meter long. The left and right  
20 sides of the aquifer were set as prescribed head conditions with hydraulic heads of 100m.  
21 Each element was assigned a hydraulic conductivity and a specific storage value using a  
22 stochastic random field generator (Gutjahr, 1989). The geometric mean of hydraulic



1 conductivity was 0.225 m/d and the geometric mean of specific storage was  $0.01 \text{ m}^{-1}$ . The  
2 variance of  $\ln K$  was 0.11 and the variance of  $\ln S_s$  was 0.1.

3 Using this one-dimensional aquifer, a pumping test was simulated at location  $x =$   
4 9.5m with a pumping rate of  $2.0 \text{ m}^3/\text{d}$ . The flow approached a steady state condition after  
5 16 days of pumping; about 95% of total drawdown occurred in the first 6 days of the  
6 pumping test. The cross correlation between head and parameters during the pumping test  
7 was then evaluated using a first-order analysis at five locations,  $x=1.5$ ,  $x=3.5$ ,  $x=5.5$ ,  
8  $x=7.5$ , and  $x= 9.5$  m. Figure 1 depicts the behavior of cross correlation between  $h$  and  $f$   
9 as a function of time at the five locations, and Figure 2 depicts the behavior of cross  
10 correlation between  $h$  and  $s$ . Each curve in the figures represents the cross correlation  
11 between head and parameter at the same location. Figure 1 shows that, in all locations,  
12 the cross correlation between  $h$  and  $f$  was low at early time and increased. Finally, it  
13 stabilized to a maximum value at a later time, around day seven. The cross correlation  
14 between  $h$  and  $s$ , however, increased sharply and reached its maximum value at an early  
15 time, only about two days, and then decreased and stabilized to its minimum value at a  
16 later time, around day thirteen (Figure 2). These results suggest that to obtain good  
17 estimates of  $f$  and  $s$  simultaneously, head information should be used that encompasses  
18 the entire pumping process -- including early time and late time.

19 The temporal correlation of transient heads was also evaluated. Figure 3 shows  
20 the contours of the temporal correlation of the head at  $x= 7.5$  m from the beginning of the  
21 pumping test to 6 days. As indicated in the figure, the heads at different times were  
22 highly correlated, especially at later time. The high correlation suggests that the heads at  
23 a given observation location at different times provide overlapping information. In

1 particular, the inclusion of heads at all time steps would be very computational time  
2 consuming for our estimator because the adjoint equations (9) and (10) must be solved  
3 once for each head observation in time. Because of the overlapping head information,  
4 choosing heads at several time steps instead of using heads at all time steps would  
5 significantly reduce the computation burdens and keep the usefulness of head information.

6       Based on the cross correlation and temporal correlation analysis, we thereafter  
7 tested our inverse approach for a well-posed inverse problem (deterministic inverse  
8 problems, Yeh et al., 1996). The head responses of all elements were collected at 0.5  
9 days, 2.5 days, and 5.5 days, representing early, middle, and late times of the pumping  
10 test, respectively. One direct hydraulic conductivity measurement and one specific  
11 storage measurement were also assumed to be known at element one (i.e., the boundary  
12 fluxes are known). As a result, the necessary and sufficient conditions for inverse  
13 modeling (i.e., the transient head responses of all elements at two time steps, as well as  
14 boundary conditions) are fully specified, (see Sun, 1996 and Yeh and Šimůnek, 2002).  
15 The inverse problem thus becomes well posed and both parameter fields can be uniquely  
16 determined. Figures 4 and 5 compare the true hydraulic conductivity field and specific  
17 storage with estimates, respectively. The comparisons indicate that our new algorithm  
18 produces accurate estimates for both parameter fields for the deterministic case, and the  
19 accuracy of our SSLE method is ensured.

20       Next, we applied transient hydraulic tomography to the one-dimensional  
21 heterogeneous aquifer to demonstrate the benefit of a hydraulic tomography test. Four  
22 locations in the one dimensional aquifer were selected as pumping and observation wells.  
23 These four wells were located at  $x=3.5\text{m}$ ,  $7.5\text{m}$ ,  $11.5\text{m}$ , and  $15.5\text{m}$ . The first pumping

1 activity was initiated at  $x = 3.5\text{m}$ , and the corresponding head responses at all four wells  
2 were recorded. The pumping rate, pumping time, and observation times were the same as  
3 the pumping test of the previous deterministic case. The three additional pumping tests  
4 had the same configuration as the first one, except the pumping was initiated at  $x = 7.5\text{m}$ ,  
5  $x = 11.5\text{ m}$ , and  $x = 15.5\text{ m}$  for the second, third, and fourth pumping test, respectively.  
6 As a result, a total of 48 head responses were collected to estimate both parameters.  
7 Comparisons of the estimated hydraulic conductivity and specific storage with true  
8 parameters are shown in Figures 6 and 7, respectively. The two figures show that, with  
9 only four head observation locations out of a total of twenty elements of entire aquifer,  
10 the hydraulic tomography with our SSLE approach produces close estimates of the true  
11 spatial patterns for both parameters. As demonstrated in Figures 6a, b, c, and d, and  
12 Figure 7a, b, c, and d, the estimates progressively improved as more head responses from  
13 tomographic pumping tests were incorporated into our SSLE approach. However, the  
14 improvement of estimates from the third to the fourth pumping test was small, which  
15 indicates that excessive pumping tests only offer negligible estimate improvements for  
16 the given number of observation wells. These findings are similar to those reported by  
17 Yeh and Liu (2000).

18

### 19 3.2 Two-Dimensional Aquifer with Nonstationary Random Property Fields

20 A common myth about geostatistical or stochastic inverse methods is that they are  
21 limited by the stationary assumption (e.g., Kosugi and Inoue, 2002). To clarify such a  
22 misunderstanding, we applied our SSLE to hydraulic tomography in a synthetic

1 nonstationary horizontal, confined aquifer. In this case, the parameters estimated in this  
2 case were transmissivity ( $T$ ) and storage coefficient ( $S$ ).

3 This aquifer was 15m long, and 15m wide and discretized into 225 elements; each  
4 element was 1m×1m. The left and right boundaries were assigned no-flow conditions  
5 while the other two sides and the initial condition were prescribed constant heads of  
6 100m. Both the transmissivity and storage coefficient varied from element to element, but  
7 were constant within one element. Both parameters were generated as nonstationary  
8 random processes using the spectral method (Gutjahr, 1989). Specifically, the aquifer  
9 was divided into four zones and both parameters in each zone had a different mean and  
10 variance from other zones (Table 1), but all the zones had the same correlation scale of 5  
11 meters in the x direction and 1 meter in the y direction. The detailed spatial distributions  
12 of both parameters are illustrated in Figures 8 and 9, respectively.

13 Nine wells (see Figure 8a for locations) were used for transient hydraulic  
14 tomography. Each pumping test lasted two days with a constant pumping rate of 1.0 m<sup>3</sup>/d.  
15 The head data at 0.4 day, 1.2 days, and 2.0 days were collected at these wells. During the  
16 estimation process, the global geometric mean of the parameter fields of the entire aquifer,  
17 not the mean for each zone, were used as input. Further, we used correlation scales of 35  
18 meters in the x direction and 5 meters in the y direction as our guess for the two  
19 parameter fields. Figure 8 and 9 show that our estimates clearly revealed the zonal  
20 structure of the aquifer and the details of heterogeneity within each zone. Therefore, our  
21 SSLE is not limited to stationary random fields—in fact, stationary or nonstationary is a  
22 subjective evaluation that varies according to the eye of the beholder.

23

### 1 3.3 Three-Dimensional Heterogeneous Aquifer

2 We subsequently applied our SSLE to transient hydraulic tomography in a  
3 synthetic three-dimensional heterogeneous confined aquifer. The geometry of this  
4 synthetic heterogeneous aquifer had dimensions of  $15\text{m} \times 15\text{m} \times 15\text{m}$ , and was  
5 discretized into 3375 elements. Each element had a uniform size of  $1\text{m} \times 1\text{m} \times 1\text{m}$ . The  
6 bottom and the top boundaries were set as no-flow, and the remaining four sides were  
7 assumed to be a prescribed hydraulic head of 100 m. A three-dimensional Cartesian  
8 coordinate system was used for spatial references. The coordinates of the bottom corner  
9 at the inner center of the cube (see Figure 10) were assigned to be (0, 0, 0) and the upper  
10 corner opposite to the bottom corner was assigned (15, 15, 15). The heterogeneous  
11 parameter fields again were generated by the spectral method (Gutjahr, 1989). The  
12 geometric mean of  $K$  was 0.34 m/d and the variance of  $\ln K$  was 0.5, while the geometric  
13 mean of  $S_s$  was  $0.0002\text{ m}^{-1}$  and the variance of  $\ln S_s$  was 0.1. The correlation scales in the  
14 x, y, and z directions were 20m, 20m, and 2m, respectively.

15 Four fully penetrating, multi-level wells were placed vertically in the aquifer. The  
16 horizontal coordinates for the four wells were (3.5, 3.5), (11.5, 3.5), (3.5, 11.5), and (11.5,  
17 11.5). Each well had seven head observation ports whose vertical coordinates were 1.5 m,  
18 3.5 m, 5.5 m, 7.5 m, 9.5 m, 11.5 m, and 13.5 m, respectively. Each well also had two  
19 pumping ports whose vertical coordinates were 4.5 m and 10.5 m, respectively. One  
20 direct hydraulic conductivity measurement and one specific storage measurement were  
21 assumed to be known at location (3.5, 3.5, 8.5). A pumping test was performed at one of  
22 the pumping ports with a constant pumping rate of  $150\text{ m}^3/\text{d}$ . The pumping test was  
23 simulated for 0.01 day with a time step of 0.0005 day. The head responses at all 28

1 observation points were monitored at time 0.002 day, 0.006 day, and 0.01 day. Seven  
2 additional pumping tests were simulated, using the same pumping rate and pumping time  
3 period, but different pumping ports. A total of 672 head observations were used in our  
4 SSLE approach to simultaneously estimate hydraulic conductivity and specific storage.

5 The SSLE was implemented on a parallel computing platform using the LINUX  
6 operating system; the interpretation of the hydraulic tomography tests was carried out  
7 using a 10-node PC cluster (Pentium 4 2.8 GHz CPU each); the total computing time for  
8 the interpretation was 610 minutes.

9 Figures 10 a, b, c, and d plot the estimated hydraulic conductivity after two, four,  
10 six, and eight pumping tests, respectively, and the true hydraulic conductivity field is  
11 shown in Figure 10e. The estimated specific storage fields after two, four, six, and eight  
12 pumping tests are illustrated in Figures 11a, b, c, and d with the true field shown in  
13 Figure 11e. Both figures 10 and 11 demonstrate that the estimates from the first two  
14 pumping tests already have captured the general pattern of heterogeneity of the aquifer;  
15 the final estimates after eight pumping tests revealed greater details, although the  
16 improvement of the estimates decreased as more pumping tests were conducted.

17 Figure 12a is a scatterplot of true hydraulic conductivity values versus those  
18 estimated after eight pumping tests and Figure 12b is the scatterplot of true specific  
19 storage values versus estimated ones. According to these figures, our estimates were  
20 unbiased with some variance, which is expected since the inverse problem is not well  
21 posed (underdetermined). Notice that the axes of both figures are log scale. The results  
22 were also quantitatively evaluated using the average absolute error norm L1 and the  
23 mean-square error norm L2, defined as:

$$1 \quad L1 = \frac{1}{n} \sum_{i=1}^n |\hat{\chi}_i - \chi_i|, \quad L2 = \frac{1}{n} \sum_{i=1}^n (\hat{\chi}_i - \chi_i)^2 \quad (12)$$

2 where  $\hat{\chi}$  and  $\chi$  are estimated and true parameters, respectively, and  $n$  is the number of  
 3 elements. The changes of L1 and L2 with increasing number of pumping tests are shown  
 4 in Figures 13a and b for hydraulic conductivity and specific storage, respectively. As  
 5 more pumping tests were added, the values of L1 and L2 decreased, but the rate of  
 6 reduction diminished. These results have the same trend as we found in the one-  
 7 dimensional case.

8 Robust as they are, neither the hydraulic tomography nor our SSLE is a perfect  
 9 method. The more head observations are collected, the higher the resolution of the  
 10 estimates will be (i.e., there is no optimal). Inaccurate head observations and hydraulic  
 11 property measurements (i.e., noises) during hydraulic tomography unequivocally can lead  
 12 to an inaccurate estimate or stability of the estimate. While our SSLE can overcome the  
 13 impacts of noise, the estimates become smooth, which means there is a loss of  
 14 effectiveness of information. These issues have been discussed in Yeh and Liu (2000).

15

#### 16 **4 Conclusions**

17 The three synthetic cases show that transient hydraulic tomography is a promising  
 18 and viable tool for detecting detailed spatial variations of hydraulic parameters with a  
 19 limited number of wells. Our SSLE can provide unbiased estimates of multiple  
 20 parameters simultaneously, and reveal their detailed spatial distributions for both  
 21 stationary and nonstationary random hydraulic property fields. In addition, our SSLE  
 22 permits sequential inclusion of head data from different pumping tests, such that the size  
 23 of the covariance matrix is small and can be solved with relative ease. By using a loop-

1 iteration scheme, our new SSLE improves estimates throughout the loops and maximizes  
2 the usefulness of head information.

3         The cross-covariance analysis reveals that the cross correlation between head and  
4 hydraulic parameters varies temporally during a pumping test. The cross correlation  
5 between head and specific storage is high at early time, while the cross correlation  
6 between head and hydraulic conductivity is high at a later time because of constant head  
7 boundary conditions that facilitate steady flow. To simultaneously estimate hydraulic  
8 conductivity and specific storage parameters, the head information used in the inverse  
9 modeling needs to include both early and late times.

10         The transient heads are highly temporally correlated, especially at later times.  
11 Such a temporal correlation structure allows our SSLE to use only a few selected heads at  
12 some time steps, instead of all available heads at all time steps, to reduce computational  
13 cost, while keeping the usefulness of the head information.

14         Our SSLE approach involves backward calculation of adjoint equations during  
15 the sensitivity analysis for transient flow. For the same number of observation locations, a  
16 transient pumping test generates much more head information than a steady state  
17 pumping test. Even when head data are used for only a few selected time steps, instead of  
18 all time steps, the computational burden of transient hydraulic conductivity is  
19 significantly greater than steady state hydraulic tomography. Our SSLE approach is  
20 implemented on a parallel platform to ease the computational burden, such that the  
21 simulation time is reduced.

22

23 **5 Acknowledgement**



1           The work reported was supported by NSF/SERDP grant #EAR-0229717 and NSF  
2 #IIS-0431079. Our gratitude is also is extended to Tim Corely and Martha P.L. Whitaker  
3 for technical editing.

4

1 **References:**

- 2 Bohling, G. C., X. Zhan, J. J. Butler Jr., and L. Zheng, Steady shape analysis of  
3 tomographic pumping tests for characterization of aquifer heterogeneities, *Water Resour.*  
4 *Res.*, 38(12), 1324, doi:10.1029/2001WR001176, 2002.
- 5 Brauchler, R., R. Liedl, and P. Dietrich, A travel time based hydraulic tomographic  
6 approach, *Water Resour. Res.*, 39(12), 1370, doi:10.1029/2003WR002262, 2003
- 7 Butler, J. J., Jr., and W. Z. Liu, Pumping tests in nonuniform aquifers: the radially  
8 asymmetric case, *Water Resour. Res.*, 29(2), 259–269, 1993.
- 9 Gottlieb, J., and P. Dietrich, Identification of the permeability distribution in soil by  
10 hydraulic tomography, *Inverse Probl.*, 11, 353–360, 1995.
- 11 Gutjahr, A., Fast Fourier transforms for random field generation, *N. M. Tech. Proj. Rep.*  
12 *Contract 4-R58-2690 R*, N. M. Inst. of Min. and Technol., Socorro, 1989.
- 13 Hanna, S., and T.-C. J. Yeh, Estimation of co-conditional moments of transmissivity,  
14 hydraulic head, and velocity fields, *Adv. Water Resour.*, 22(1), 87–95, 1998.
- 15 Hughson, D. L., and T.-C. J. Yeh, An inverse model for three-dimensional flow in  
16 variably saturated porous media, *Water Resour. Res.*, 36(4), 829–839, 2000.
- 17 Jacob, C. E., Determining the permeability of water-table aquifers, in *Methods of*  
18 *Determining Permeability, Transmissibility, and Drawdown*, compiled by R. Bentall, U.S.  
19 Geol. Surv. Water Supply Pap., 1536-I, 245–271, 1963.
- 20 Kitanidis, P. K., Parameter uncertainty in estimation of spatial functions-Bayesian-  
21 analysis, *Water Resour. Res.*, 22(4): 499-507, 1986.
- 22 Kitanidis, P. K., Quasi-linear geostatistical theory for inversing. *Water Resour. Res.*,  
23 31(10), 2411–2419, 1995.

- 1 Kosugi, K., and M. Inoue, Estimation of hydraulic properties of vertically heterogeneous  
2 forest soil from transient matric pressure data, *Water Resour. Res.*, 38(12), 1322,  
3 doi:10.1029/2002WR001546, 2002.
- 4 Li, B., and T.-C. J. Yeh, Sensitivity and moment analysis of head in variably saturated  
5 regimes, *Adv. Water Resour.*, 21(6), 477–485, 1998.
- 6 Li, B., and T.-C. J. Yeh, Cokriging estimation of the conductivity field under variably  
7 saturated flow conditions, *Water Resour. Res.*, 35(12), 3663–3674, 1999.
- 8 Liu, S., T.-C. J. Yeh, and R. Gardiner. Effectiveness of hydraulic tomography: sandbox  
9 experiments. *Water Resour. Res.* 38(4): 10.1029/2001WR000338, 2002
- 10 Liu, S., and T.-C. J. Yeh, An integrative approach for monitoring water movement in the  
11 vadose zone, *Vadose Zone Journal*, 3:681–692 (2004).
- 12 Marquardt, D. W., An algorithm for least squares estimation of non-linear parameters, *J.*  
13 *Soc. Ind. Appl. Math.*, 2, 431– 441, 1963.
- 14 McDermott CI, M., Sauter, and R. Liedl, New experimental techniques for pneumatic  
15 tomographical determination of the flow and transport parameters of highly fractured  
16 porous rock samples, *Journal of Hydrology*, 278 (1-4): 51-63 JUL 25 2003.
- 17 McLaughlin, D. and L. R. Townley, A reassessment of the groundwater inverse problem,  
18 *Water Resour. Res.* 32(5),1131–1162, 1996.
- 19 Nowak, W, and O. A. Cirpka, A modified Levenberg-Marquardt algorithm for quasi-  
20 linear geostatistical inversing , *Adv. Water Resour.*, 27 (7): 737-750 JUL 2004.
- 21 Renshaw, C.E., Estimation of fracture zone geometry from steady-state hydraulic head  
22 data using iterative sequential cokriging, *Geophysical Research Letters* 23(19): 2685-  
23 2688 SEP 15 1996.

- 1 Srivastava, R. and T.-C. J. Yeh, A three-dimensional numerical model for water flow and  
2 transport of chemically reactive solute through porous media under variably saturated  
3 conditions, *Advances in Water Resources*, 15, 275-287, 1992.
- 4 Sun, N.-Z., and W. W.-G. Yeh, A stochastic inverse solution for transient groundwater  
5 flow: Parameter identification and reliability analysis, *Water Resour. Res.*, 28(12), 3269–  
6 3280, 1992.
- 7 Sykes, J. F., J. L. Wilson and R. W. Anderews, Sensitivity analysis for steady state  
8 groundwater flow using adjoint operators, *Water Resour. Res.*, 21(3), 359-371, 1985.
- 9 Tikhonov, A. N., and V. Y. Arsenin, *Solutions of Ill-Posed Problems*, Halsted Press/  
10 Wiley, New York, 1977.
- 11 Vargas-Guzman, A. J., and T.-C. J. Yeh, Sequential kriging and cokriging: two powerful  
12 geostatistical approaches, *Stochastic Environ.Res. Risk Assess.*, 13, 416–435, 1999.
- 13 Vargas-Guzman, A. J., and T.-C. J. Yeh, The successive linear estimator: a revisit, *Adv.*  
14 *Water Resour.*, 25, 773-781, 2002.
- 15 Vasco, DW, H, Keers, and K. Karasaki, Estimation of reservoir properties using transient  
16 pressure data: An asymptotic approach, *Water Resour. Res.*, 36 (12): 3447-3465, Dec.  
17 2000.
- 18 Wu, C-M, T-C. J. Yeh, T-H. Lee, N-S Hsu, C-H Chen, A. F. Sancho, Traditional aquifer  
19 tests: comparing apples to oranges? *Water Resour. Res.*, in review.
- 20 Yeh, T.-C. J., Stochastic modeling of groundwater flow and solutetransport in aquifers, *J.*  
21 *Hydrol. Processes*, 6, 369–395, 1992.
- 22 Yeh, T.-C.J., A. L. Gutjahr, and M.H. Jin, An iterative cokriging-like technique for  
23 ground water flow modeling, *Ground Water*, 33(1), 33-41, Jan.-Feb. 1995.

- 1 Yeh, T.-C. J., M. Jin, and S. Hanna, An iterative stochastic inverse approach: conditional  
2 effective transmissivity and head fields, *Water Resour. Res.*, 32(1), 85-92, 1996.
- 3 Yeh, T.-C., and J. Zhang, A geostatistical inverse method for variably saturated flow in  
4 the vadose zone, *Water Resour. Res.*, 32(9), 2757–2766, 1996.
- 5 Yeh, T.-C. J., Scale issues of heterogeneity in vadose-zone hydrology, in *Scale*  
6 *Dependence and Scale Invariance in Hydrology*, edited by G.Sposito, Cambridge Univ.  
7 Press, New York, 1998.
- 8 Yeh, T.-C. J., and S. Liu, Hydraulic tomography: Development of a new aquifer test  
9 method, *Water Resour. Res.*, 36(8), 2095–2105, 2000.
- 10 Yeh, T. -C. J. and J. Šimůnek, Stochastic fusion of information for characterizing and  
11 monitoring the vadose zone, *Vadose Zone Journal*, Vol. 1, p 207-221, 2002
- 12 Yeh, T.-C. J., S. Liu, R. J. Galss, K. Baker, J.R. Brainard, D. Alumbaugh, and D.  
13 LaBrecque, A geostatistically based inverse model for electrical resistivity surveys and its  
14 applications to vadose zone hydrology, *Water Resour. Res.*, 38(12), 1278, doi:  
15 10.1029/2001WR001204, 2002.
- 16 Yeh, W. W-G, Review of parameter-identification procedures in groundwater hydrology  
17 - the inverse problem, *Water Resour. Res.*, 22 (2): 95-108, 1986.
- 18 Zhang, J., and T.-C. J. Yeh, An iterative geostatistical inverse method for steady flow in  
19 the vadose zone, *Water Resour. Res.*, 33(1), 63–71, 1997.

20

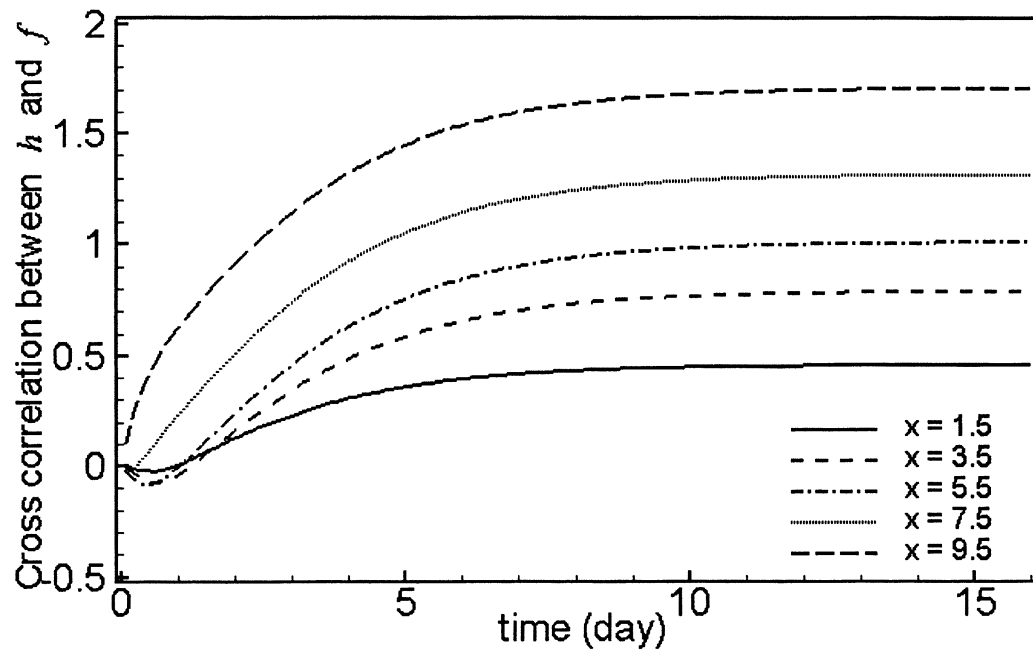
21

22

23

Table 1: Statistical properties of the nonstationary aquifer

	Geometric mean of transmissivity ( $m^2/d$ )	Variance of $\ln$ transmissivity	Geometric mean of Storage coefficient	Variance of $\ln$ Storage coefficient
zone 1	0.250	0.150	0.001	0.040
zone 2	0.030	0.110	0.008	0.080
zone 3	0.320	0.121	0.002	0.009
zone 4	0.040	0.120	0.007	0.060

Figure 1. Cross correlation between  $h$  and  $f$  as a function of time during a pumping test.

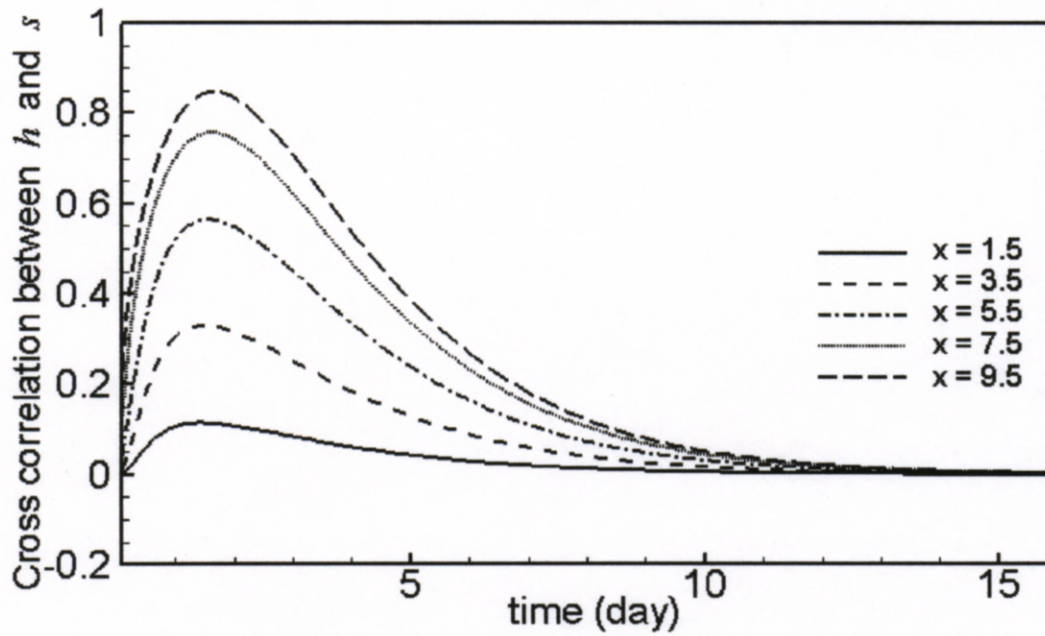


Figure 2. Cross correlation between  $h$  and  $s$  as a function of time during a pumping test.

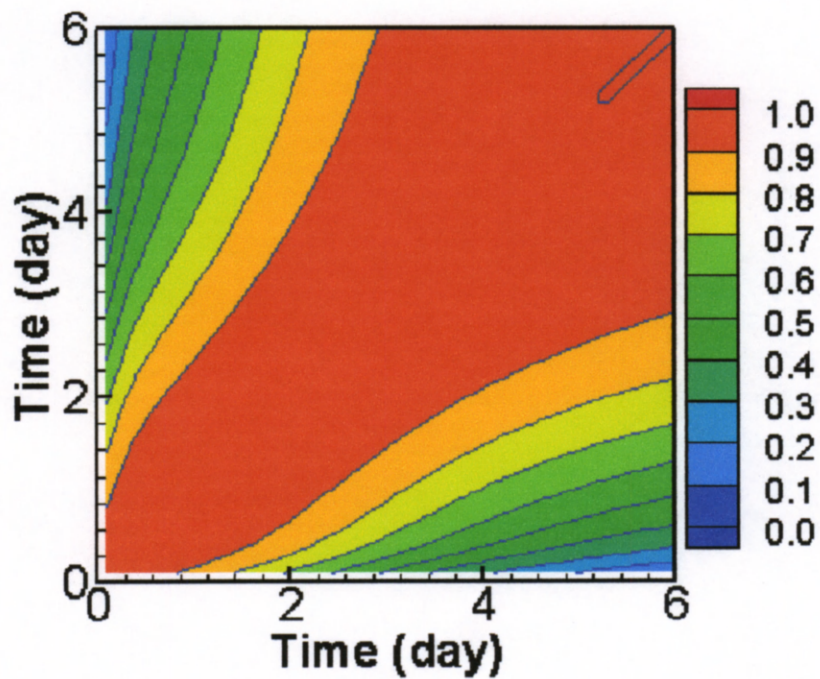


Figure 3. Temporal correlation of transient heads at  $x = 7.5$  m during a pumping test.

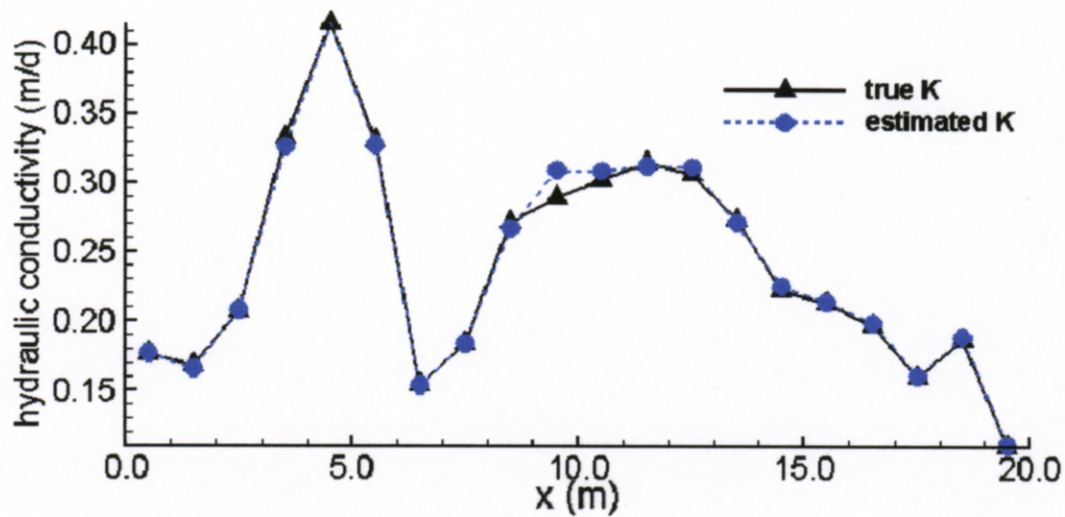


Figure 4. Comparison of estimated hydraulic conductivity with true hydraulic conductivity in a deterministic case.

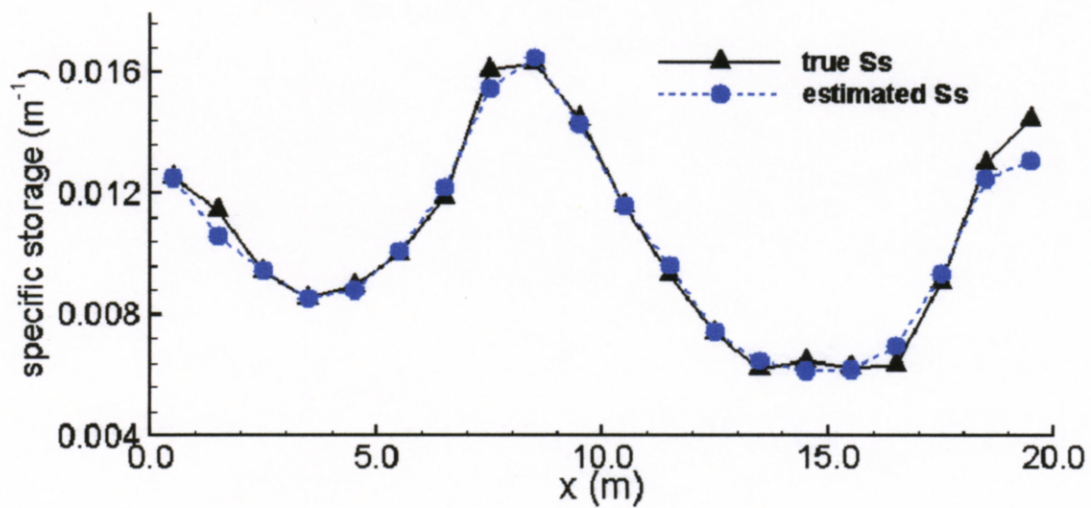


Figure 5. Comparison of estimated specific storage with true specific storage in a deterministic case.



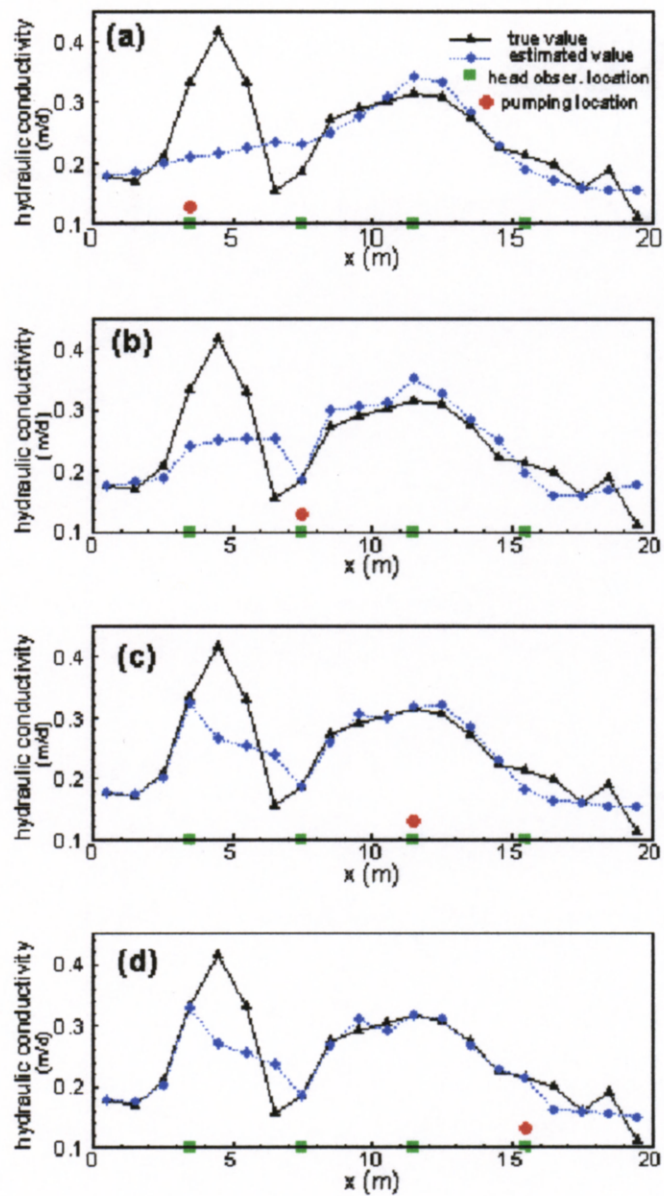


Figure 6 Estimated hydraulic conductivity from transient hydraulic tomography (a) estimates from the first pumping test; (b) estimates from the additional second pumping test; (c) estimates from the additional third pumping tests; (d) estimates from the four pumping tests.

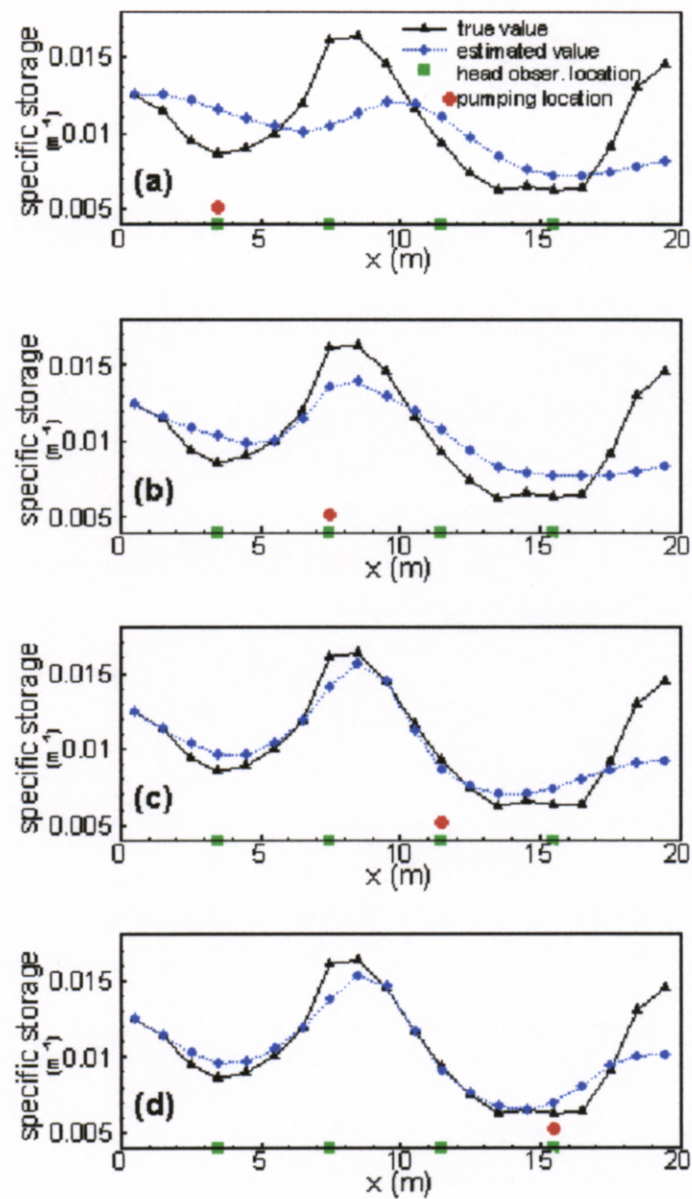


Figure 7 Estimated specific storage from transient hydraulic tomography (a) estimates from the first pumping test; (b) estimates from the additional second pumping tests; (c) estimates from the additional third pumping tests; (d) estimates from the fourth pumping tests.



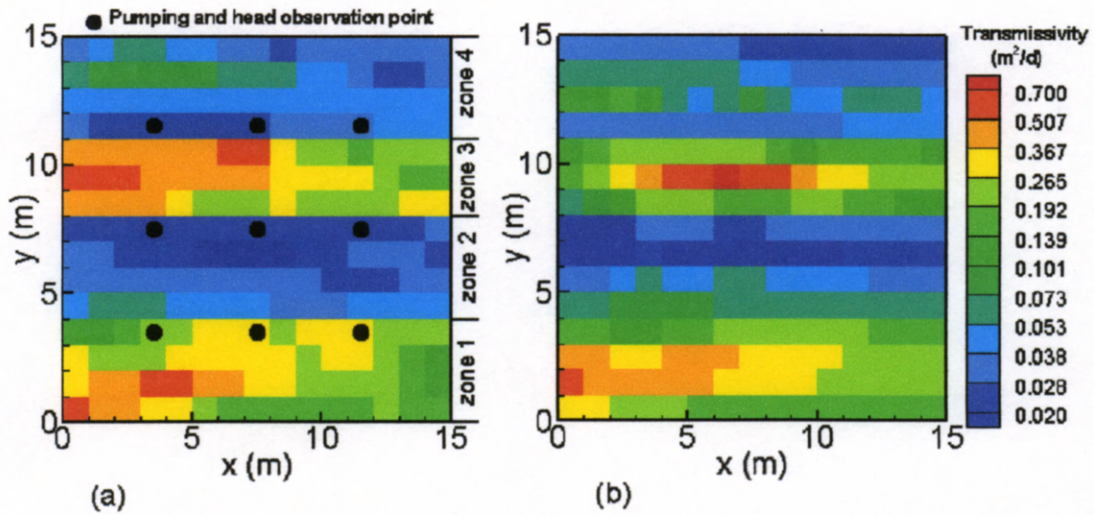


Figure 8 Comparison between (a) true transmissivity field and (b) estimated transmissivity field for a 2-D aquifer with nonstationary hydraulic properties.

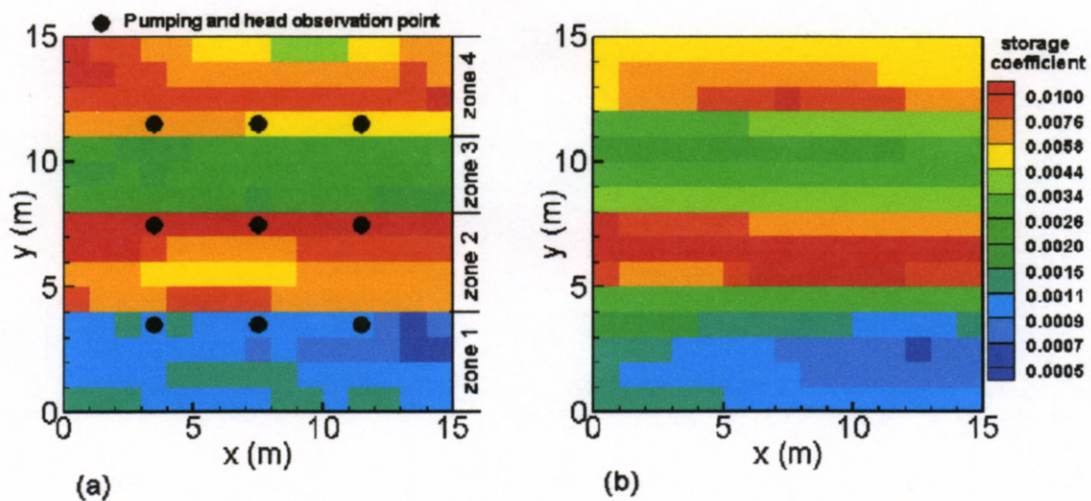


Figure 9 Comparison between (a) true storage coefficient field and (b) estimated storage coefficient field for a 2-D aquifer with nonstationary hydraulic properties.

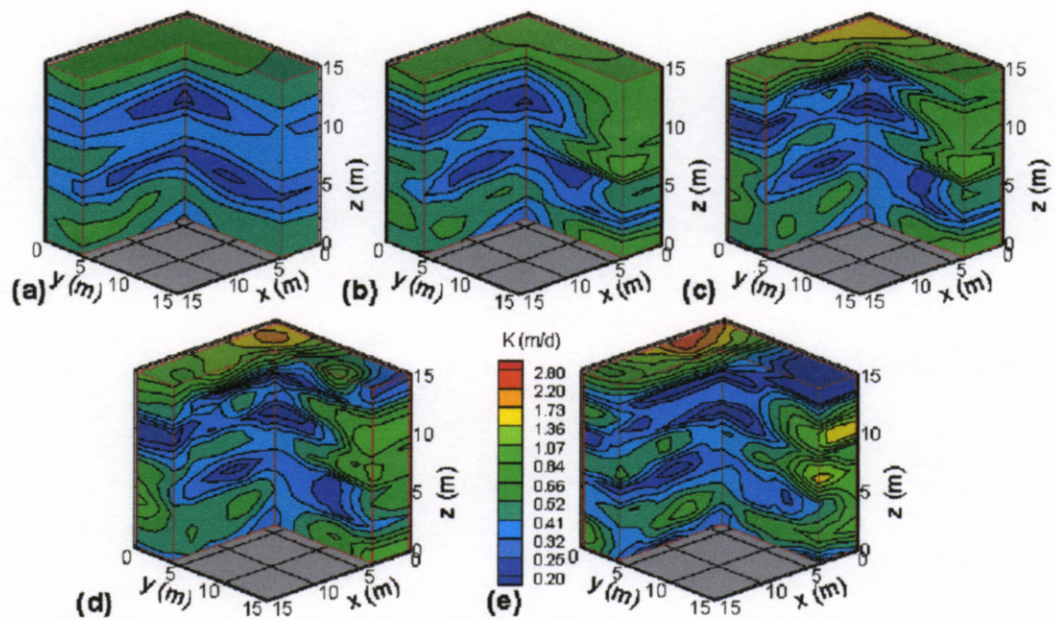


Figure 10 Comparison between estimated hydraulic conductivity with the true field in a three dimensional aquifer: estimated hydraulic conductivity field after (a) two, (b) four, (c) six, (d) and eight pumping tests, and (e) the synthetic true hydraulic conductivity field.



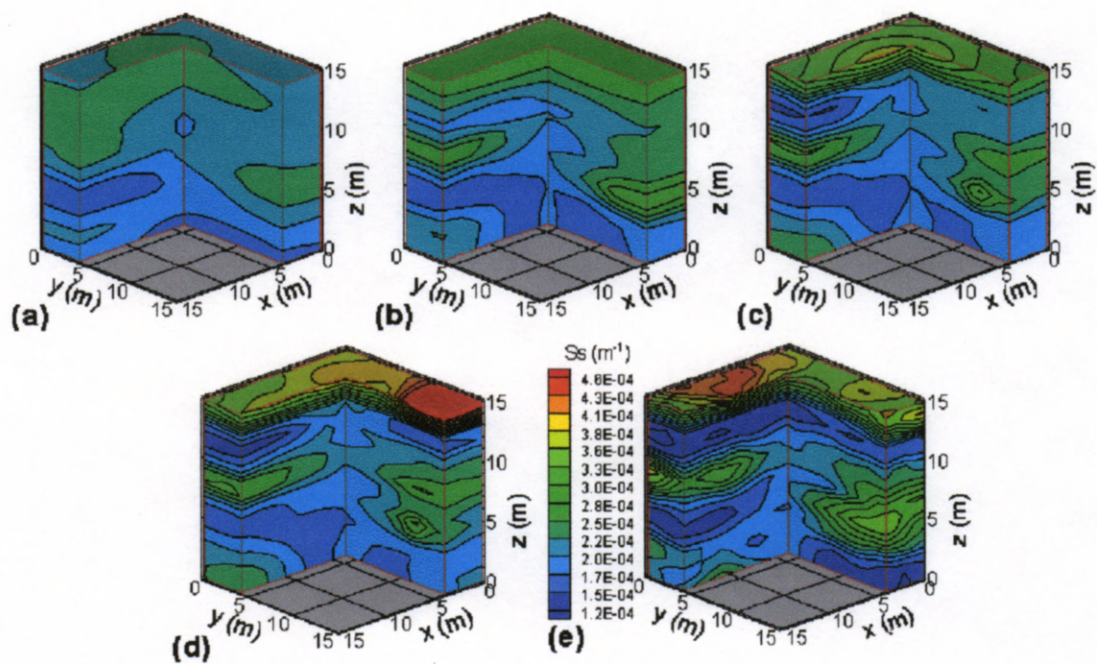


Figure 11. Comparison between estimated specific storage with the true field in a three dimensional aquifer: estimated specific storage field after (a) two, (b) four, (c) six, (d) and eight pumping tests, and (e) the synthetic true hydraulic conductivity field.

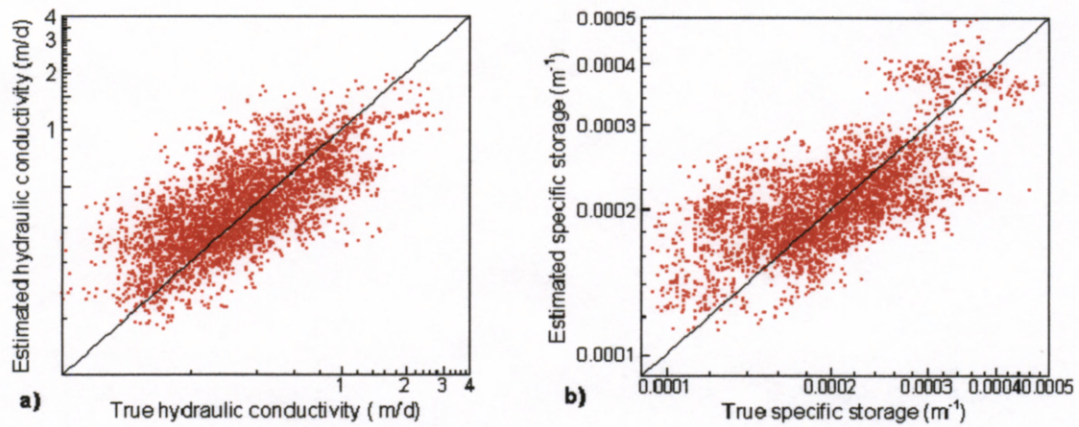


Figure 12. Scatterplots of a) estimated vs. true hydraulic conductivity; b) estimated vs. true specific storage.

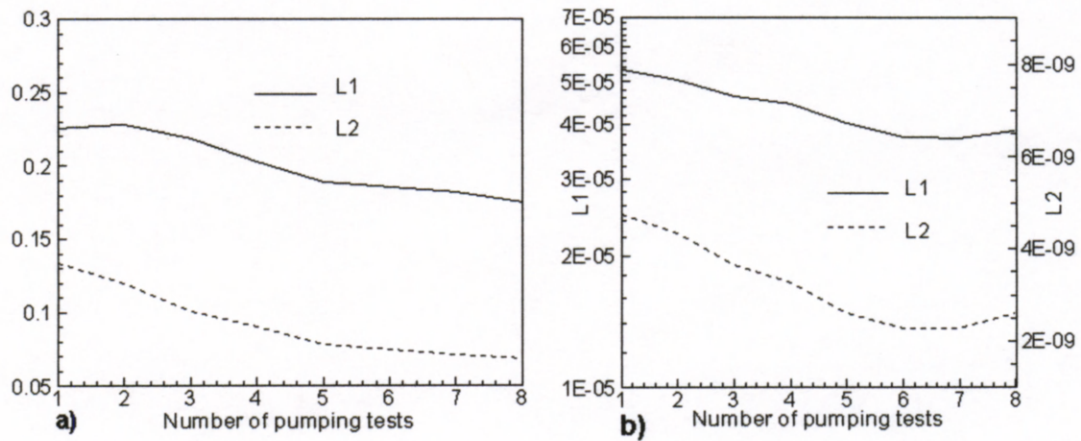


Figure 13. Statistical norms of our estimates: a) hydraulic conductivity; b) specific storage.